ASTROBIOLOGY
Volume 15, Number 10, 2015

DOI: 10.1089/ast.2015.1301

The Archean Nickel Famine Revisited

Kurt O. Konhauser,[1] Leslie J. Robbins,[1] Ernesto Pecoits,[1,2] Caroline Peacock,[3]
Andreas Kappler,[4] and Stefan V. Lalonde[5]

Abstract

Iron formations (IF) preserve a history of Precambrian oceanic elemental abundance that can be exploited to examine nutrient limitations on early biological productivity. However, in order for IF to be employed as paleomarine proxies, lumped-process distribution coefficients for the element of interest must be experimentally determined or assumed. This necessitates consideration of bulk ocean chemistry and which authigenic ferric iron minerals controlled the sorption reactions. It also requires an assessment of metal mobilization reactions that might have occurred in the water column during particle descent and during post-depositional burial. Here, we summarize recent developments pertaining to the interpretation and fidelity of the IF record in reconstructions of oceanic trace element evolution. Using an updated compilation, we reexamine and validate temporal trends previously reported for the nickel content in IF (see Konhauser *et al.*, 2009). Finally, we reevaluate the consequences of methanogen Ni starvation in the context of evolving views of the Archean ocean-climate system and how the Ni famine may have ultimately facilitated the rise in atmospheric oxygen. Key Words: Methane—Biogeochemistry—Chemical evolution—Iron formation—Archean. Astrobiology 15, 804–815.

1. Introduction

It was proposed that a nickel (Ni) famine at the end of the Archean caused a catastrophic collapse of atmospheric methane (CH_4) that then allowed for the rise of atmospheric oxygen (Konhauser *et al.*, 2009). This hypothesis was based on the secular trend in molar Ni/Fe ratios in iron formations (IF) that recorded a reduced flux of dissolved Ni to seawater *ca.* 2.7 billion years ago. By determining Ni partitioning coefficients between simulated Precambrian seawater and diverse iron oxyhydroxides, it was concluded that dissolved Ni concentrations may have reached $\sim$400 n*M* throughout much of the Archean but dropped below $\sim$200 n*M* by 2.5 Ga. As Ni is a key metal cofactor in several enzymes of methanogens, its decline would have stifled their activity in the ancient marine water column and sediments, disrupting the supply of biogenic methane. It was suggested that a depressed biogenic methane supply would have facilitated the accumulation of oxygen in the atmosphere, leading to the so-called ''Great Oxidation Event'' (GOE) some 2.45 billion years ago (Konhauser *et al.*, 2011).

Within the past 5 years, that hypothesis has been questioned on two grounds. The first is that the partitioning coefficients used to extrapolate dissolved Ni concentrations in the Precambrian oceans may have been underestimated because they did not consider that the initial ferric iron phase could have been green rust (Zegeye *et al.*, 2012). This impacts extrapolated paleoseawater Ni concentrations, as green rust sorbs Ni more efficiently than the precursor ferric hydroxide phase, such as ferrihydrite ($Fe[OH]_3$), necessitating lower equilibrium dissolved Ni concentrations to explain the IF data. The second is that Ni may have been remobilized from ferrihydrite during the particles' descent through the water column and upon burial (Frierdich *et al.*, 2011). If Ni was lost from the particles, then what is recorded in IF is only a fraction of what might initially have been deposited. These two critiques operate in opposite directions, implicating either lower Ni (in the case of a green rust sorbent) or higher Ni (in the case of diagenetic Ni loss) in Archean seawater than that estimated by Konhauser *et al.* (2009).

In this work, we had three objectives. First, we provide an updated Ni/Fe database expanded by 676 filtered data

[1]Department of Earth and Atmospheric Sciences, University of Alberta, Edmonton, Canada.
[2]Equipe Géobiosphère, Institut de Physique du Globe-Sorbonne Paris Cité, Université Paris Diderot, CNRS, Paris, France.
[3]School of Earth and Environment, University of Leeds, Leeds, UK.
[4]Geomicrobiology, Center for Applied Geoscience, Eberhard-Karls-University Tuebingen, Tuebingen, Germany.
[5]CNRS-UMR6538 Laboratoire Domaines Océaniques, European Institute for Marine Studies, Technopôle Brest-Iroise, Plouzané, France.

points, nearly two-thirds greater than what was available at the time of the original study (1085), to determine whether the initial trends in Ni/Fe ratios through time are conserved in the expanded data set. Second, we discuss how recent experimental studies on IF mineral precipitation and diagenesis bear on the utility of the IF trace metal record as a proxy for evolving Precambrian seawater composition. Third, we incorporate evolving views of the Archean ocean-climate system to paint a more complete picture of oxygen's rise during the GOE.

2. Nickel Concentrations in Precambrian IF and Archean Seawater

After updating the IF compilation of Ni/Fe by nearly 700 points (Fig. 1), the trends shown here demonstrate a remarkable fidelity to those first described by Konhauser *et al.* (2009). A dramatic decline in Ni between 2.7 and 2.5 Ga remains clear. When combined with the distribution coefficients obtained from Konhauser *et al.* (2009), this updated record would still indicate a paleomarine Ni concentration of up to $\sim$400 n*M* in the Archean. Following the precipitous drop in Ni, concentrations would approach $\sim$200 n*M* by 2.5 Ga, with modern levels established by the Neoproterozoic. It is encouraging that the first-order, secular trends in paleomarine Ni concentrations preserved in the IF record are also recorded by other proxy records, such as sedimentary to early diagenetic pyrite (Large *et al.*, 2014).

An alternative way to evaluate paleomarine Ni concentrations from IF data without using experimentally derived partition coefficients is by examining the scaling between Ni and Fe in the IF record itself (Fig. 2). In doing so, it becomes apparent that there is a correlation between Fe and Ni deposition; that is, as Fe increases so too does Ni, as expected for partition coefficient-type behavior of Ni sorption to Fe minerals. On such a cross plot, we may also superimpose the scaling expected between a trace metal and Fe based on hypothesized partitioning scenarios (*cf.* Robbins *et al.*, 2013). The advantage of this approach is that hypothesized partitioning scenarios can be overlain on the IF record data and subsequently evaluated. If the hypothesized partitioning is reflective of the actual deposition of IF minerals, then the proposed lines should constrain the majority of IF data. Indeed, when the K_D values predicted by Konhauser *et al.* (2009) are superimposed on the cross plot (Fig. 2), almost the entire range of Ni/Fe values in the IF record fall within the predicted ranges. This concordance does not attest to the accuracy or reality of experimentally determined K_D values, as the slope in solid-phase Ni versus Fe space is calculated as K_D*$[Ni]_{sw}$ and thus depends equally on $[Ni]_{sw}$. In the case of the Konhauser *et al.* (2009) partitioning scenarios, $[Ni]_{sw}$ values were originally extrapolated from the rock record data using experimentally determined K_D values, such that the presented K_D*$[Ni]_{sw}$ scenarios (slopes in Ni vs. Fe space) are necessarily tuned to this data set, and apparent correspondence may be considered circular. However, what Fig. 2 effectively demonstrates is (1) that partitioning scenarios can be readily evaluated against rock record data, and should be in order to be considered tenable, and (2) that looking forward, supposedly free parameters (K_D, $[Ni]_{sw}$) could conceivably be tuned against rock record data to explore plausible scenarios in K_D-$[Ni]_{sw}$ space, as was done by Robbins *et al.* (2013) for Zn/Fe in the absence of experimentally determined partition coefficients.

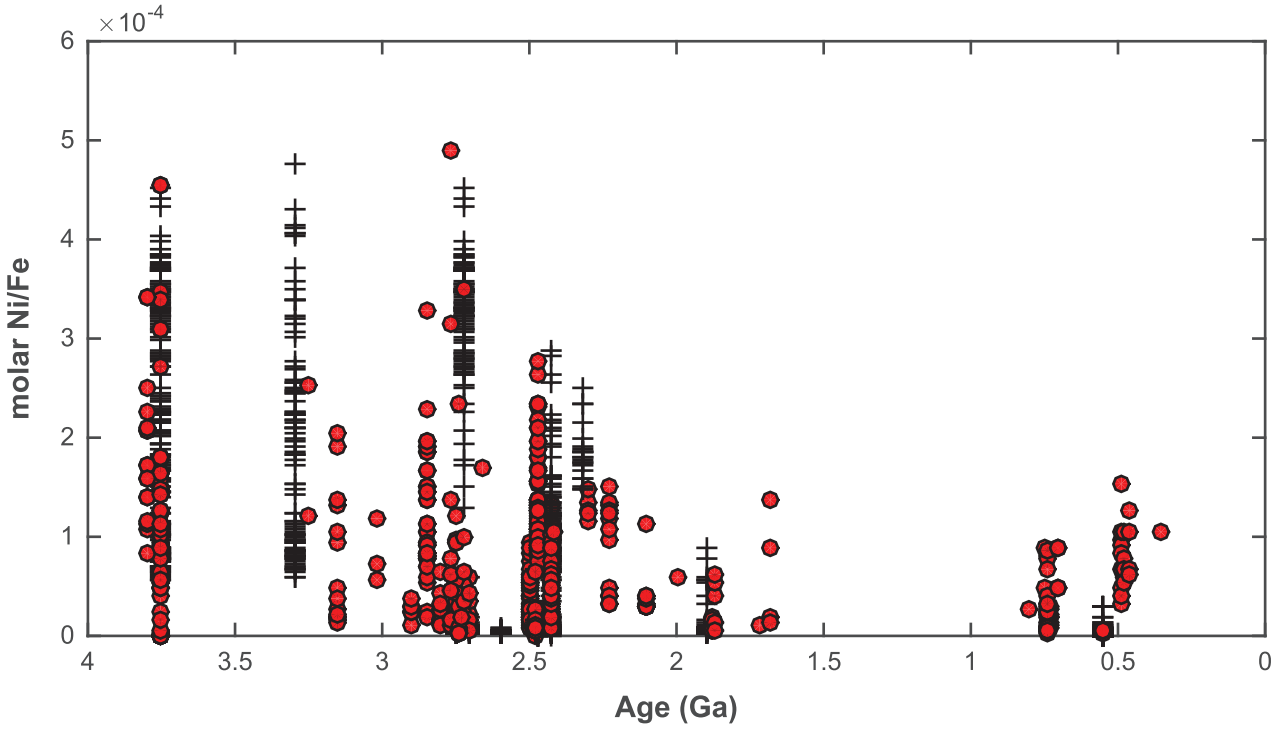

FIG. 1. Compilation of Ni/Fe ratios in IF through time; this reflects an updated version of Fig. 1 in the work of Konhauser *et al.* (2009) with an additional 676 new analyses. Crosses indicate laser ablation analyses of individual grains, and red circles bulk-digest data. (Color graphics available at www.liebertonline.com/ast)

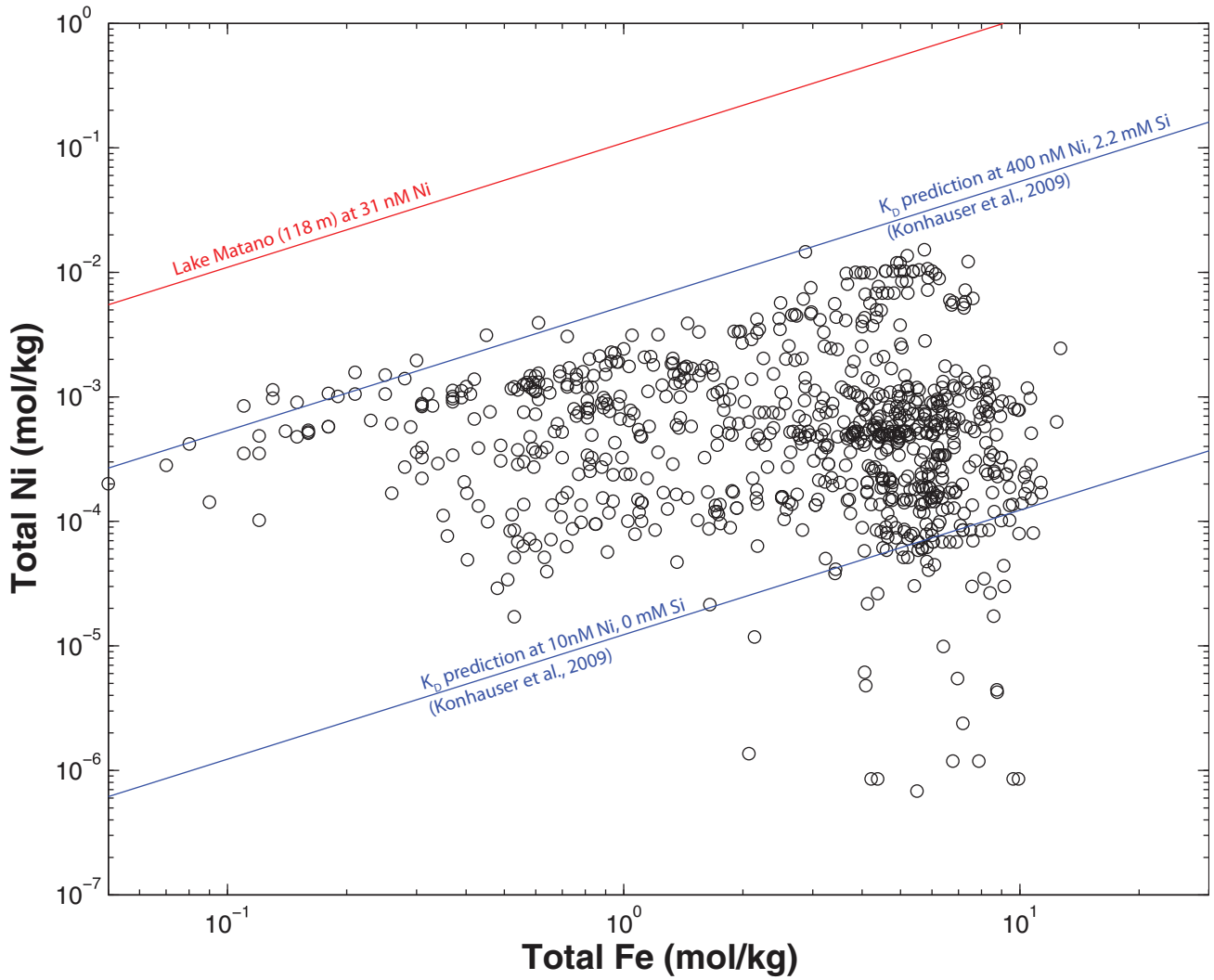

FIG. 2. Ni-Fe cross plot showing partitioning of Ni as recorded by IF. Blue lines indicate the anticipated scaling of Ni with Fe based on the partitioning scenarios of Konhauser *et al.* (2009). Also shown as a red line is the anticipated scaling based on the partitioning scenario determined for green rust in Lake Matano (Zegeye *et al.*, 2012). (Color graphics available at www.liebertonline.com/ast)

An important consideration in using the IF record to extrapolate the paleomarine concentrations of trace elements is the influence of organic carbon. The reason being that it is becoming increasingly accepted that microorganisms were in some way involved in the primary oxidation of dissolved Fe(II) to the precursor ferrihydrite particles (Konhauser *et al.*, 2007a; Pecoits *et al.*, 2015). Two possible roles for bacteria are envisioned. The original model of biological IF precipitation assumed the oxidation of hydrothermal Fe(II), via abiotic oxidation by any available O_2 generated through oxygenic photosynthesis, that is, cyanobacteria (Cloud, 1972; Klein and Beukes, 1989), and/or via biotic oxidation by chemolithotrophic bacteria, that is, microaerophilic Fe(II)-oxidizers, such as the genera *Gallionella* (Holm, 1989). Phototrophic Fe(II)-oxidizing bacteria (the so-called photoferrotrophs) were discovered two decades ago (Widdel *et al.*, 1993) and represent an attractive pathway for explaining early IF precipitation in the absence of O_2 (Ehrenreich and Widdel, 1994; Heising *et al.*, 1999; Posth *et al.*, 2008, 2013a; Köhler *et al.*, 2010; Pecoits *et al.*, 2015). These bacteria fix CO_2 phototrophically using Fe^{2+} as an electron donor, potentially generating large quantities of Fe(III) in the process. The attractiveness of this concept is that it explains IF deposition in the absence of molecular oxygen using dissolved Fe^{2+} that would have been abundant in seawater at that time, and they would have been capable of oxidizing enough Fe(II) to explain even the largest IF deposits (Konhauser *et al.*, 2002). In fact, calculations based on experimentally determined Fe(II)-oxidation rates by these organisms under light regimes representative of ocean water at depths of a few hundred meters suggest that, even in the presence of cyanobacteria, anoxygenic phototrophs living beneath a wind-mixed surface layer would have had the first opportunity to utilize Fe^{2+} (Kappler *et al.*, 2005).

If the precursor ferrihydrite was biologically generated, then it stands to reason that organic carbon may have influenced Ni sorption to the precursor ferrihydrite particles. For instance, it has been shown that biogenic ferrihydrite, consisting of cell-mineral aggregates, differs from abiogenic

minerals in terms of chemical composition, particle size, and density (Posth *et al.*, 2010), as well as surface sorptive properties (Moon and Peacock, 2012, 2013; Muehe *et al.*, 2013). To this end, Eickhoff *et al.* (2014) examined the partitioning of Ni to both abiogenic and biogenic ferrihydrite. In these experiments, the biogenic ferrihydrite consisted of a cell-mineral aggregate precipitated by either a freshwater or marine photoferrotroph. When normalized to specific surface area, biogenic ferrihydrite sorbed less Ni, apparently due to microbially derived organics or whole cells binding to the mineral surface and thereby competing with Ni for sorption sites. Eickhoff *et al.* (2014) suggested that, given the potential for co-precipitating organic matter to depress partitioning of Ni, (i) previous estimates for Ni concentrations in Archean seawater may be too low, and (ii) the decline of Ni in Precambrian ocean may have occurred closer to the GOE, at 2.45 Ga. However, comparing the data from Eickhoff *et al.* (2014) to those presented by Konhauser *et al.* (2009) requires caution. While Konhauser *et al.* (2009) used a concentration of Fe (0.179 m*M*) plausible for Archean oceans (Fe: 0.02–0.5 m*M*, Holland, 1973; Morris, 1993), the concentrations used in the Eickhoff study were constrained by experimental limitations; a concentration of 2 m*M* Fe(II) was used for microbial Fe(II) oxidation to grow enough cells for a visualization by scanning transmission X-ray microscopy (STXM), and 10 mg/L (170 μM) Ni was required for STXM analysis (Hitchcock *et al.*, 2009), a factor of 400 greater than the values extrapolated by Konhauser *et al.* (2009) and $\sim 10^4$ greater than modern seawater. Using these particular concentrations excludes a Si/Fe ratio relevant for Archean oceans, which makes it difficult to draw direct conclusions about partitioning of Ni considering the strong inhibitory role Si appears to play during trace element sorption to ferrihydrite (Konhauser *et al.*, 2007b, 2009).

In addition to considerations based on the presence of silica and organic matter, others have suggested that IF may have been dominated by precursor mineral phases other than ferrihydrite with significantly different Ni sorption behavior. Based on field observations from the stratified and ferruginous water column in Lake Matano in Indonesia, Zegeye *et al.* (2012) suggested that carbonated green rust constituted an important shuttle for water column Ni to lakebed sediments. From their data, they suggested that green rust is three times more efficient at sorbing Ni compared to ferrihydrite. When considering this possibility, and its applicability to the interpretation of the IF record, several factors must be considered. First, green rust is not an abundant ferric iron precipitate today. At modern marine hydrothermal vents (*e.g.*, Loihi) and in acid mine drainage settings, where Fe(II) oxidation is widespread, the dominant ferric oxyhydroxide mineral precipitated is ferrihydrite, with lesser amounts of goethite (*e.g.*, Toner *et al.*, 2012, and Clark *et al.*, 1997, respectively). Green rust occurs only as a transient phase during the experimental formation and reduction of ferric oxyhydroxides (*e.g.*, Cornell and Schwertmann, 2003, and Parmar *et al.*, 2001, respectively) and Fe(II) oxidation by some nitrate-reducing bacteria (Pantke *et al.*, 2012), as well as in some soils (*e.g.*, Trolard *et al.*, 1997), and at the transitional boundary in Lake Matano (Zegeye *et al.*, 2012), but it is certainly not abundant in nature. Second, there is no direct evidence to support the formation of green rust in the Precambrian oceans, other than potentially as a transient phase, despite the ocean composition being fundamentally different than today. Recent work on the IF record has supported the assertion that the primary precipitates forming IF were likely ferric oxyhydroxides, in particular ferrihydrite (Ahn and Buseck, 1990; Bekker *et al.*, 2010; Sun *et al.*, 2015), although a recent study by Rasmussen *et al.* (2015) suggests that the primary precipitates comprised a ferrous-ferric silicate phase, such as greenalite. The Fe-isotope signatures of some Archean and Proterozoic IF suggest a biogenic or abiogenic Fe-oxide or oxyhydroxide mineral phase, rather than green rust, ankerite, or siderite (Planavsky *et al.*, 2012). Third, both freshwater and marine photoferrotrophs that oxidize Fe(II) during anoxygenic photosynthesis and may have been ultimately responsible for iron formation generally produce poorly crystalline ferrihydrite, even under fully anoxic conditions (*e.g.*, Kappler and Newman, 2004; Eickhoff *et al.*, 2014; Wu *et al.*, 2014). Fourth, when the partitioning coefficients of Zegeye *et al.* (2012) are evaluated in the face of Ni/Fe ratios preserved in the IF record, there is an obvious and fundamental disconnect with respect to the partitioning scenario occurring in Lake Matano (Fig. 2). Dissolved Ni concentrations at the studied depths in Lake Matano (31–50 n*M*) are broadly comparable to modern oceanic values ($\sim$10 n*M*). However, if the partitioning scenarios observed in Lake Matano were applied to the IF record, Archean Ni concentrations would have to have been some 100–1000 times lower than modern oceanic values. This scenario is difficult to reconcile with the general secular evolution of both Earth's crust and sediments from Ni-rich to Ni-poor over geological time (Konhauser *et al.*, 2009).

The authors attribute this disconnect in part to the deficiency of silica in Lake Matano (300–420 μM; Crowe *et al.*, 2008) relative to Precambrian oceans, whose presence results in depressed Ni sorption (Konhauser *et al.*, 2009). The experimental partitioning data of Konhauser *et al.* (2009), performed for several different silica concentrations (670 μM, saturation with respect to cristobalite, and 2200 μM, saturation with respect to amorphous silica), indicate that dissolved silica at levels approaching saturation with respect to amorphous silica suppresses Ni sorption by a factor of approximately 10 in terms of the K_D value relative to the silica-free condition (0.00123 μM^{-1} at 2.20 m*M* Si versus 0.01341 μM^{-1} at 0 m*M* Si; Konhauser *et al.*, 2009). This highlights the necessity for considering elevated silica concentrations when examining the partitioning of Ni into Fe minerals. Furthermore, Jones *et al.* (2015) estimated Precambrian silica concentrations on the order of 600–1500 μM, the lower end being not too dissimilar to concentrations currently present in Lake Matano. Thus, the presence or absence of silica alone does not appear to account for the drastic difference in Ni sorption efficiency between green rust in Lake Matano and synthetic ferrihydrite. Further experiments are warranted, but the simplest explanation may be that green rust played little role in trace element shuttling during Archean IF deposition.

3. Nickel Mobility during Diagenesis

One potentially troubling aspect regarding the interpretation of the IF record of evolving paleomarine Ni is the

secondary mobilization of Ni from the ferrihydrite-rich sediments during burial. In this regard, Frierdich *et al.* (2011) suggested that IF were unsuitable proxies for Ni concentrations through time as interactions with Fe(II)-rich fluids could have stimulated the release of Ni; this is a function of redox-driven recrystallization of Fe minerals exposed to ferrous iron. For instance, Frierdich and Catalano (2012) experimentally showed a release of 2.0% and 11.2% of Ni from hematite and goethite, respectively, when Ni-substituted minerals reached equilibrium with Fe(II) solutions. A greater magnitude of release was observed when Ni-substituted hematite and goethite were sequentially exposed to fresh Fe(II) solutions every 2 weeks for up to seven cycles. Under this scenario, 6.6% and 27.6% of Ni were released from hematite and goethite, respectively. When IF are considered open systems, as in the work of Frierdich *et al.* (2011) and Frierdich and Catalano (2012), then it is certainly possible that the IF record only a fraction of the initially sorbed Ni. Importantly, this implies that the resultant paleomarine concentrations extrapolated from the K_D values determined by Konhauser *et al.* (2009) would be too low and that decreases in the marine Ni reservoir over time were even more dramatic than as originally proposed by Konhauser *et al.* (2009).

If we consider the upper and lower limits of Ni release observed, 27.6% and 2%, respectively, we can apply a correction factor to the Ni/Fe ratios in the IF record, in order to account for this loss. Considering these two extremes, a factor of between 1.38 and 1.02 can be surmised. In the case of 27.6% of Ni being mobilized, this would be the equivalent to dividing either the Ni or Ni/Fe value from the respective analyses by 0.724 (*i.e.*, $1/0.724 = 1.38$) or multiplying by the corresponding correction factor (*i.e.*, 1.38). Conceptually, this would treat the IF record as representing only 72.4% of the initial Ni, with the other 27.6% being mobilized, prior to the application of a correction factor. Accordingly, this factor becomes lower when one considers that less Ni is mobilized, converging to 1.00 as the amount mobilized decreases. Given that the Ni record in IF shows $\sim 40\times$ decrease in paleomarine-dissolved Ni concentrations from the Precambrian to the modern, a correction factor between 1.38 and 1.02 imparts relatively little difference. For example, at 400 n*M* Ni, the highest concentrations predicted for the Archean by Konhauser *et al.* (2009), the corrected concentration becomes 552 n*M*. If anything this would imply that the previous estimate of Konhauser *et al.* (2009) and those presented in this article are more conservative than previously argued, a possibility in line with the work of Eickhoff *et al.* (2014) discussed above.

It is crucial to point out that experiments reacting Ni-substituted Fe-minerals with Fe(II) solutions (*e.g.*, Frierdich *et al.*, 2011; Frierdich and Catalano, 2012) were performed in trace element–free solutions. This is a situation far removed from ferrihydrite forming in equilibrium with seawater or subsequently transforming in contact with sediment pore-waters. When precipitating particles sorb Ni in a similar manner to K_D experiments, particle composition (and correspondingly, Ni/Fe ratios) are determined by equilibrium with surrounding fluids. Placing Ni-substituted hematite or goethite into a Ni-free Fe(II) solution represents a system at disequilibrium and would clearly promote mobilization of Ni by leaching. The importance of this can be viewed by comparing the mobilization of Ni by Fe(II) solutions when the fluid is periodically replaced and when the solution remains unchanged over the length of the experiment (Frierdich and Catalano, 2012). This comparison suggests that the magnitude of Ni mobilized is significantly reduced when some Ni is present. Once Ni is released from either goethite or hematite, the Fe(II) solutions reach equilibrium with the mineral phases, and no further release of Ni is observed. Under such a case only ~ 2–11% of Ni is mobilized and, viewed in light of the IF record, has little effect on extrapolated paleomarine Ni concentrations. Furthermore, this redox-driven recrystallization becomes more complicated when impurities in the minerals are considered. Frierdich *et al.* (2012) showed that the mobilization of Ni is attenuated when the mineral structure contains other impurities, such as Sn, Al, or Cr; this scenario is more realistic in terms of Fe particles precipitating in the Precambrian oceans and sinking to the bottom sediments to ultimately become IF.

The remobilization of Ni from IF sediment has been recently examined in a set of experiments designed to consider diagenetic mineral transformation. As discussed above, given the likely catalytic role that microbes played in Fe(II) oxidation during IF precipitation, the organic remains and ferric oxyhydroxide particles would together have settled through the water column and become deposited at the seafloor (*e.g.*, Li *et al.*, 2011). Given that the bulk water column was anoxic, perhaps with the exception of an upper layer of oxygenated waters above the chemocline of a stratified ocean (*e.g.*, Klein and Beukes, 1989), ferrihydrite would have represented a favorable electron acceptor for the oxidation of the cellular remains. Coupling the reduction of Fe(III) minerals to the oxidation of organic matter not only explains the low content of organic carbon in the IF (<0.5%; Gole and Klein, 1981), but it also explains the prevalence of light carbon isotope compositions in associated carbonate minerals (Perry *et al.*, 1973; Walker, 1984; Baur *et al.*, 1985), the light iron isotope compositions of magnetite and siderite (*e.g.*, Johnson *et al.*, 2008; Craddock and Dauphas, 2011), and the textures of the reduced iron phases (*e.g.*, Kolo *et al.*, 2009; Köhler *et al.*, 2013; Y.-L. Li *et al.*, 2013). In this regard, Posth *et al.* (2013b) and Köhler *et al.* (2013) both demonstrated that by incubating ferrihydrite at 1.2 kbar and 170°C for 14 days the mineralogical transition from ferrihydrite to hematite is complete. The addition of organic carbon to these diagenetic experiments led to the formation of reduced Fe minerals in the post-diagenetic capsules, mainly a mixture of hematite, magnetite, and siderite, a composition broadly consistent with the modern-day mineralogy of IF.

Robbins *et al.* (2015) took this one step further, demonstrating that, during these diagenetic mineral transformations, Ni remains largely immobile. In fact, more than 91% of Ni was retained following the mineral transformations characteristic of these diagenetic experiments. Post-diagenetic analysis of the particles indicated a mineralogy dominated by hematite with Ni strongly retained in the particles. Critically, those experiments captured the dehydration of ferrihydrite to hematite, which can occur at temperatures below 140°C (Becker and Clayton, 1976). Ni was retained on both biogenic ferrihydrite and abiogenic ferrihydrite, in the presence and absence of glucose. Both biogenic ferrihydrite and abiogenic ferrihydrite, in the

presence of glucose, should provide ideal conditions for Fe(III) reduction and mobilization of Ni via redox-driven reactions. When considered alongside other evidence for authigenic seawater signatures in IF, such as the preservation of marine-like rare earth element (REE) patterns (*e.g.*, Bau and Dulski, 1996; Bolhar *et al.*, 2004; Hofmann, 2005; Pecoits *et al.*, 2009; Haugaard *et al.*, 2013), these findings suggest IF should be a robust indicator of paleomarine concentrations, and by extension Ni/Fe ratios, even after diagenetic mineral transformations. Moreover, $\delta^{18}O$ isotope heterogeneity in BIF hematite grains is thought to reflect near-primary depositional features, and clearly contrasts with the limited range of O isotope compositions in quartz, which are best explained by homogenization through recrystallization and exchange with secondary fluids (W. Li *et al.*, 2013). Similarly, Fe isotope heterogeneity between hematite and magnetite layers is interpreted to reflect variable extents of oxidation and precipitation from aqueous Fe(II) of variable isotopic composition, depending on the proportion of hydrothermal versus diagenetic input, and as such, are considered not to have been overprinted by post-depositional processes (Frost *et al.*, 2006; Steinhoefel *et al.*, 2010; Y.-L. Li *et al.*, 2013).

Finally, it is important to stress that the observations made by Konhauser *et al.* (2009) were based on temporal trends, that is, changing dissolved Ni concentrations in seawater from the Archean through to the present. Irrespective of whether extrapolated paleomarine Ni concentrations were overestimated (*e.g.*, Zegeye *et al.*, 2012) or underestimated (Frierdich *et al.*, 2011; Frierdich and Catalano, 2012; Eickhoff *et al.*, 2014), the key observation is the drop in dissolved Ni concentrations between 2.7 and 2.5 Ga and the fact that Ni concentrations in IF prior to 2.7 Ga were never reached again. The IF record is clear on this, suggesting that the authigenic marine nature of this signal remains undisputed. Suppressed methanogenesis remains a likely outcome of diminishing Ni concentrations in seawater (see section below).

4. Archean Methanogen Famine Revisited

It has been postulated that, as long as biogenic methane production was high, oxygen could not accumulate in the atmosphere because of the high chemical reactivity of the two gases (*e.g.*, Zahnle *et al.*, 2006). In their model, oxidative weathering of terrestrial sulfide minerals increased the supply of dissolved sulfate (SO_4^{2-}) to the oceans, which in turn facilitated the ecological success of sulfate-reducing bacteria (SRB) over methanogens by around 2.4 Ga. Moreover, anaerobic oxidation of methane by sulfate would have further reduced methane escape with increasing sulfate concentrations at that time (Catling *et al.*, 2007). However, it is not until after the GOE that evidence in the rock record exists for pervasive oxidative weathering of terrestrial sulfides, a large oceanic sulfate pool, and the onset of widespread ocean euxinia (*e.g.*, Poulton *et al.*, 2004). Konhauser *et al.* (2009) provided an alternative hypothesis suggesting that the demise in large-scale methanogenesis occurred prior to, and not necessarily related to, increasing environmental oxygenation. That model provided a clear directionality in the evolution of Earth's system, whereby a cooler mantle after 2.7 Ga led to associated chemical changes in volcanism and trace element abundances in the oceans, triggering a decline in global methanogenesis and ultimately facilitating the transition from anoxic to oxic atmospheric conditions some 2.4 billion years ago.

Without question, much of the nickel famine hypothesis rests on the assumption that methane levels were high in the Archean (*e.g.*, Kasting and Siefert, 2002) and in some way a determinant for the timing of the rise of atmospheric oxygen. Although abiogenic supplies of methane were likely minimal during the Hadean due to a relatively high early mantle oxygen fugacity (*e.g.*, Wade and Wood, 2005), when methanogenic bacteria evolved, perhaps as early as 4.1 Ga (Battistuzzi *et al.*, 2004), they provided a flux of methane sufficient to sustain an atmospheric CH_4 mixing ratio of $>10^{-3}$, or some 1000 times that of today (Pavlov *et al.*, 2000). Evidence for biogenic methane accumulation exists in Paleoarchean chert-hosted fluid inclusions (Ueno *et al.*, 2006) and in marine sediments, where $\delta^{13}C_{org}$ values of Neoarchean kerogen are often lower than $-40‰$ and can reach $-60‰$ (Eigenbrode and Freeman, 2006). Such isotopically light marine organic matter either reflects the primary productivity of methanogens (*e.g.*, Londry *et al.*, 2008), incorporation of methane into biomass of methanotrophic bacteria (Hayes *et al.*, 1983), or the formation of a ^{12}C-enriched organic haze by photolysis of methane (Pavlov *et al.*, 2001).

Our initial hypothesis also necessitates that seawater Ni concentrations did indeed decline after 2.7 Ga. This view has merit because a hotter Archean mantle (*e.g.*, Berry *et al.*, 2008) led to more mantle source melting, which produced abundant Ni-rich komatiite and olivine-rich basalt as new seafloor, seamounts, and continental crust (*e.g.*, Kamber *et al.*, 2005). Second, Archean tholeiites, which make up most of the oceanic crust, were richer in Ni than modern tholeiites ($\sim$140 vs. $\sim$90 ppm; Arndt, 1991). Third, a major peak in preserved komatiite abundance occurred during the most intense period of mantle plume magmatism and continental crustal growth recorded in Earth's history, between 2.72 and 2.66 Ga (Condie, 1998; Barley *et al.*, 2005), after which their abundance decreased rapidly. Ultimately, the hotter Archean mantle produced more Ni-rich ultramafic rocks, resulting in a much greater supply of Ni to the oceans than any time thereafter (Smithies *et al.*, 2005).

Perhaps it is no coincidence that the demise of methanogens and the rise of cyanobacteria are linked. In a competition for resources, if one microorganism does well, the others are held in check through competitive exclusion (*e.g.*, Hibbing *et al.*, 2010; Weber *et al.*, 2014). Microbes can further enhance their competitiveness through the production of antimicrobial compounds or by having evolved a better resistance to some external chemical. In the case of methanogens, although no studies to date have shown any pathogenic species, they do have toxin/antitoxin systems (Cavicchioli *et al.*, 2003), while a study of acidic peat bogs showed that the addition of the antibiotic rifampicin inhibited growth of acetogens without affecting the growth of methanogens (Bräuer *et al.*, 2004). In either case, it is possible that methanogens pre-2.7 Ga were widely dispersed throughout the oceans, from below the photic zone of the water column to the bottom sediments, with photoautotrophs dominating the surface. Based on the predicted iron:phosphorous (Fe:P) ratios in evolving Precambrian upwelling waters, Jones *et al.* (2015) suggested that photoferrotrophs would likely have faired better than the cyanobacteria as long

as the oceans were highly ferruginous (with Fe:P >424, as based on the Redfield ratio), but as soon as dissolved Fe:P fell below 424, iron would be exhausted, leaving P to fuel other modes of photoautotrophy, such as oxygenic photosynthesis. Similarly, Swanner *et al.* (2015) experimentally demonstrated that highly ferruginous waters were toxic to cyanobacteria because high Fe^{2+} concentrations caused intracellular reactive oxygen species to accumulate within the cell, leading to decreased photosynthetic efficiency and lower growth rates. Rampant methanogenesis, whether supported by higher H_2 fluxes or organic matter produced by anoxygenic phototrophy, would have contributed to the maintenance of the largely anoxic conditions. In turn, this permitted widespread Fe(II) dispersal that would have prevented cyanobacterial proliferation should the Fe(II)-related brakes identified by Jones *et al.* (2015) and Swanner *et al.* (2015) prove critical.

In addition to the drop in seawater Ni concentrations after 2.7 Ga, other events around this time would have converged to cause a contraction in methanogens while simultaneously facilitating the rise of cyanobacteria. First, the increasing supply of solutes and sediments from weathering of the newly emergent continents (*e.g.*, Lalonde and Konhauser, 2015) led to the formation of stable continental platforms. This, in turn, facilitated the diversification of stromatolites that utilized these shallow-water settings (McNamara and Awramik, 1992) and the evolution of new types of cyanobacteria with greater motility and faster growth rates, which could better compensate for continuous accretion (Knoll, 1984). With increased consumption of CO_2, indiscriminate sedimentation of massive amounts of calcium carbonate took place *in situ* on the seafloor, leading to decimeter- to meter-thick beds that extended over thousands of square kilometers (Grotzinger and Knoll, 1999). Moreover, increased nutrient supply would also have had the effect of increasing the productivity of planktonic cyanobacteria, as envisioned for increased phosphorus delivery to the ocean following the snowball Earth glaciations in the Neoproterozoic (Planavsky *et al.*, 2010). The end result was that cyanobacteria now expanded throughout the shallow littoral zones, and the oxygen they produced would have marginalized the methanogens that were already in decline.

Second, there should have been waning fluxes of H_2 (methanogen's preferred reductant) to the bulk ocean waters with decreasing serpentinization of the seafloor (*i.e.*, $2Mg_{1.8}Fe_{0.2}SiO_4 + 2.933H_2O \rightarrow Mg_{2.7}Fe_{0.3}Si_2O_5(OH)_4 + 0.9Mg(OH)_2 + 0.033Fe_3O_4 + 0.033H_2$), accompanying the decrease in production of olivine-rich oceanic crust at the end of the 2.7 Ga mantle plume event and the concomitant growth and stabilization of continental cratons (Barley *et al.*, 2005). Kump and Barley (2007) argued that the shift from predominantly submarine volcanism to more subaerial volcanism further decreased abiotic H_2 fluxes since the latter yield more oxidized gases (H_2O, CO_2, and SO_2). A loss of H_2 would likely have contributed to a declining biogenic methane supply (Kharecha *et al.*, 2005) even if methanogens continued to grow directly on seafloor crust—as they do today—where the source of both Ni and H_2 remained locally abundant (*e.g.*, Brazelton *et al.*, 2006; Amend *et al.*, 2011).

Third, seawater concentrations of Fe^{2+} declined episodically on the shallow regions of the continental shelves due to the cessation of plume-driven submarine volcanism and a lowering of sea level. On the semi-restricted carbonate platforms, such as that represented by the *ca.* 2.65–2.46 Ga Campbellrand Subgroup in South Africa, lower concentrations of Fe^{2+} allowed for ''oxygen oases'' to develop. In fact, stromatolites persist on kilometer-scale outcrops, suggestive of an active marine biosphere (Sumner, 1997). The presence of dissolved oxygen in seawater along the slope is inferred based on shifts toward heavier $\delta^{15}N$ values in shale organic carbon that are consistent with the onset of an oxic N cycle (Godfrey and Falkowski, 2009), varying abundances in rhenium (Re) and molybdenum (Mo) in shales that reflect cycling of these elements in oxygenated seawater (Kendall *et al.*, 2010), and coupled Fe and Mo isotopes that indicate the formation of ferric oxyhydroxides in the upper water column that were likely linked to cyanobacteria rather than photoferrotrophs (Czaja *et al.*, 2012). The platform had rimmed margins (Sumner and Beukes, 2006), which could have sheltered cyanobacteria in lagoons from the delivery of Fe(II)-rich water that was sourced from depth, based on the deposition of Fe-rich shales along the slope and IF deeper in the basin (Klein and Beukes, 1989). Geochemical indicators of oxygen appear during a sea-level regression, but disappear during transgressions (Godfrey and Falkowski, 2009), and are temporally limited, lasting perhaps tens of millions of years (Sumner and Beukes, 2006).

The transition from a methane-dominated ocean to a cyanobacteria-dominated ocean is perhaps best evidenced in the 150-million-year section (2.72–2.57 Ga) of late Archean shallow- and deep-water sediments of the Hamersley Basin in Western Australia. Eigenbrode and Freeman (2006) reported $\delta^{13}C_{org}$ values for 175 kerogen samples, with a range of values between −57‰ and −28‰. The most isotopically depleted kerogens are from the oldest samples, and the magnitude of their depletion is best accounted for by the biological processes of methane assimilation and oxidation. Methane oxidation requires electron acceptors, such as O_2, nitrate (NO_3^-), or SO_4^{2-}, with the latter two indirectly requiring O_2 to form the oxidized species, although Fe(III) has also been hypothesized (*e.g.*, Konhauser *et al.*, 2005) and shown experimentally (Beal *et al.*, 2009) to oxidize methane, and as such, methanotrophy could in principal not be linked to O_2. Nonetheless, highly ^{13}C-depleted kerogens at 2.72 Ga, as well as the recovery of methylhopane biomarkers indicative of aerobiosis (Eigenbrode *et al.*, 2008), point to the availability of both methane and oxygen at that time. It is also interesting to note that a $\delta^{13}C_{org}$ shift of 29‰ in the kerogens occurs in shallow-water carbonates (evolving from −57‰ to −28‰) over that time compared to only 5‰ (−45‰ to −40‰) in the deep-water sediments. These patterns are interpreted as reflecting a gradual transition in shallow waters of a microbial habitat strongly influenced by methane cycling at 2.72 Ga to one more influenced by oxygenic photosynthesis by 2.57 Ga (Hayes *et al.*, 1983; Eigenbrode and Freeman, 2006; Eigenbrode *et al.*, 2008); cyanobacteria tend to fractionate carbon by 32–25‰ (*e.g.*, Popp *et al.*, 1998), while anoxygenic phototrophs fractionate to a lesser degree (*e.g.*, Robinson *et al.*, 2003). In deeper settings, kerogen remained highly ^{13}C-depleted, indicating that these environments continued to be dominated by methanogenic-methanotrophic communities and were not yet influenced by the major changes in carbon cycling taking place in shallow waters. By comparing the Hamersley data to those reported elsewhere, Eigenbrode and Freeman

(2006) further suggested that ''a global-scale expansion of oxygenated habitats accompanied the progression away from anaerobic ecosystems toward respiring microbial communities fuelled by oxygenic photosynthesis before the oxygenation of the atmosphere 2.45 billion years ago.''

As the GOE commenced *ca.* 2.45 Ga, aerobic chemolithoautotrophic weathering of pyrite on land produced significant acidity, which would have increased sulfate and nutrient fluxes to seawater (Reinhard *et al.*, 2009; Konhauser *et al.*, 2011). With increased sulfate supply to the oceans, marine SRB would have begun to dominate the anoxic regions of the water column, leading to the further marginalization of methanogens to the sulfate-poor bottom sediments, as is the case today. The end result of the progressive decline in methane production (a potent greenhouse gas) was a cooling climate, eventually culminating in the onset of major Paleoproterozoic glaciations (Zahnle *et al.*, 2006).

Kasting (2013) suggested that a decline in methanogenesis could not have led to the progressive oxidation of Earth's surface. According to his model, if the methane that was being produced originated from atmospheric H_2 (Reaction 4), then a decrease in methanogenesis should have decreased atmospheric total hydrogen mixing ratio, thereby decreasing both H_2 loss and O_2 production. If the methane instead originated from fermentation and methanogenesis within seafloor sediments, the net reaction would have been as in Reaction 5. Each mole of CH_4 that was produced should have led to 2 mol of escaping H_2 (Reaction 6; see Catling *et al.*, 2001), but the 2 mol of CH_2O that would have been buried had the methanogens not been there would have been the equivalent of 4 mol of H_2 escaping (see Kasting, 2013, Reaction 10); thus O_2 production is again decreased. So, according to Kasting (2013), this mechanism cannot have contributed to the rise of atmospheric O_2.

$$[4] \quad CO_2 + 4H_2 \rightarrow CH_4 + 2H_2O$$

$$[5] \quad 2CH_2O \rightarrow CH_4 + CO_2$$

$$[6] \quad CH_4 + h\nu \rightarrow C + 2H_2$$

This model makes two assumptions whose validity is worth examining. First, in the case of H_2-driven methanogenesis, it is assumed that atmospheric H_2 is consumed that would have otherwise contributed to the total atmospheric mixing ratio of hydrogen. If instead volcanic or mantle H_2 tended to be fixed in organic matter (for example, by photoferrotrophy; Croal *et al.*, 2009) and buried without methanogenesis, the net effect would be to prevent the transfer of H_2 and CH_4 to the atmosphere, such that methanogenesis becomes an important driver of hydrogen escape, not a brake (Catling *et al.*, 2001). The second assumption, for the case of CH_2O methanogenesis, is related in that the reducing power that generated the organic matter undergoing methanogenesis comes at the expense of atmospheric H_2. If methanogenesis releases the equivalent of 2 mol H_2 to the atmosphere to participate in hydrogen escape, but its absence results in the burial of 4 mol H_2 equivalents that would not otherwise contribute to hydrogen escape (for example, burial of biomass produced by non-H_2-based phototrophy), then burial is the more efficient pathway for generating oxidizing equivalents at Earth's surface, and any decrease in hydrogen escape arising from depressed methanogenesis becomes subordinate.

The landscape of possible metabolic and reactive transport scenarios is admittedly complex, and the ensemble of consequences of depressed methanogenesis in Earth's redox balance and the GOE itself warrants further scrutiny. To complicate matters, increases in primary productivity (*e.g.*, the first widespread oxygenic photosynthesis in open oceans) would stimulate methanogenesis and atmospheric methane mixing ratios, plausibly to the point of organic haze formation (Domagal-Goldman *et al.*, 2008; Zerkle *et al.*, 2012; Kurzweil *et al.*, 2013). Such a haze would be bi-stable and self-supporting by positive feedbacks, requiring a significant drop in methane fluxes to transition away from a thick haze (Zerkle *et al.*, 2012; Kurzweil *et al.*, 2013). The evolving nickel scarcity provides a directional, compelling hypothesis for why methane fluxes might drop in the face of the ramping biological productivity often evoked for the GOE.

5. Conclusion

An expanded database of Ni/Fe ratios in iron formation through geological time reaffirms a profound and unidirectional shift in nickel availability during the late Archean. Extrapolation from rock record data to paleomarine dissolved Ni concentrations in ancient seawater, for example, using partition coefficient approaches, is not necessarily straightforward; and there exist a variety of caveats, mostly pertaining to the system specificity of partition coefficient approaches (*e.g.*, mineralogy, the role of biomass and competing ions during sorption) as well as potential diagenetic effects. In reviewing these caveats, we conclude that some are not necessarily applicable to Precambrian oceans, others may have faults stemming from experimental design, while others may be of little impact to reconstructed Ni concentrations. That said, caution is welcome when extrapolating elemental concentrations from the rock record to ancient seawater, and we detail approaches for evaluating and potentially tuning trace element partitioning scenarios in light of the rock record data itself. While the biospheric effects of the nickel famine are likely multiple and more nuanced than the scenario originally envisioned by Konhauser *et al.* (2009), especially with respect to global redox balance and the possibility of organic haze in the atmosphere, all experimental and rock record evidence to date reaffirm that marine Ni concentrations dropped precipitously and unidirectionally between 2.7 and 2.5 Ga, never to recover.

Acknowledgments

Funding was provided by the National Sciences and Engineering Research Council of Canada (NSERC) to Kurt O. Konhauser; a Vanier Canada Graduate Scholarship to Leslie J. Robbins; the UnivEarthS Labex program at Sorbonne Paris Cité to Ernesto Pecoits; LabexMER to Stefan V. Lalonde; the European Research Council to Andreas Kappler; and NERC (Natural Environment Research Council) and STFC (Science & Technology Facilities Council) to Caroline Peacock.

References

Ahn, J.H. and Buseck, P.R. (1990) Hematite nanospheres of possible colloidal origin from a Precambrian banded iron formation. *Science* 250:111–113.

Amend, J.P., McCollom, T.M., Hentscher, M., and Bach, W. (2011) Catabolic and anabolic energy for chemolithoautotrophs in deep-sea hydrothermal systems hosted in different rock types. *Geochim Cosmochim Acta* 75:5736–5748.

Arndt, N.T. (1991) High Ni in Archean tholeiites. *Tectonophysics* 187:411–420.

Barley, M.E., Bekker, A., and Krapež, B. (2005) Late Archean to early Paleoproterozoic global tectonics, environmental change and the rise of atmospheric oxygen. *Earth Planet Sci Lett* 238:156–171.

Battistuzzi, F.U., Feijao, A., and Hedges, S.B. (2004) A genomic timescale of prokaryote evolution: insights into the origin of methanogenesis, phototrophy, and the colonization of land. *BMC Evol Biol* 4:1–14.

Bau, M. and Dulski, P. (1996) Distribution of yttrium and rare-earth elements in the Penge and Kuruman iron-formations, Transvaal Supergroup, South Africa. *Precambrian Res* 79:37–55.

Baur, M.E., Hayes, J.M., Studley, S.A., and Walter, M.R. (1985) Millimeter-scale variations of stable isotope abundances in carbonates from banded iron-formations in the Hamersley Group of Western Australia. *Econ Geol* 80:270–282.

Beal, E.J., House, C.H., and Orphan, V.J. (2009) Manganese- and iron-dependent marine methane oxidation. *Science* 325:184–187.

Becker, R.H. and Clayton, R.N. (1976) Oxygen isotope study of a Precambrian banded iron-formation, Hamersley Range, Western Australia. *Geochim Cosmochim Acta* 40:1153–1165.

Bekker, A., Slack, J.F., Planavsky, N., Krapež, B., Hofmann, A., Konhauser, K.O., and Rouxel, O.J. (2010) Iron formation: the sedimentary product of a complex interplay among mantle, tectonic, oceanic, and biospheric processes. *Econ Geol* 105:467–508.

Berry, A.J., Danyushevsky, L.V., O'Neill, H.C., Newville, M., and Sutton, S.R. (2008) Oxidation state of iron in komatiite melt inclusions indicates hot Archaean mantle. *Nature* 455:960–963.

Bolhar, R., Kamber, B.S., Moorbath, S., Fedo, C.M., and Whitehouse, M.J. (2004) Characterisation of early Archaean chemical sediments by trace element signatures. *Earth Planet Sci Lett* 222:43–60.

Bräuer, S.L., Yavitt, J.B., and Zinder, S.H. (2004) Methanogenesis in McLean Bog, an acidic peat bog in upstate New York: stimulation by H_2/CO_2 in the presence of rifampicin, or by low concentrations of acetate. *Geomicrobiol J* 21:433–443.

Brazelton, W.J., Schrenk, M.O., Kelley, D.S., and Baross, J.A. (2006) Methane- and sulfur-metabolizing microbial communities dominate the Lost City Hydrothermal Field ecosystem. *Appl Environ Microbiol* 72:6257–6270.

Catling, D.C., Zahnle, K.J., and McKay, C.P. (2001) Biogenic methane, hydrogen escape, and the irreversible oxidation of early Earth. *Science* 293:839–843.

Catling, D.C., Claire, M.W., and Zahnle, K.J. (2007) Anaerobic methanotrophy and the rise of atmospheric oxygen. *Philos Transact A Math Phys Eng Sci* 365:1867–1888.

Cavicchioli, R., Curmi, M.G., Saunders, N., and Thomas, T. (2003) Pathogenic archaea: do they exist? *Bioessays* 25:1119–1128.

Clark, W.A., Konhauser, K.O., Thomas, J.C., and Bottrell, S.H. (1997) Ferric hydroxide and ferric hydroxysulfate precipitation by bacteria in an acid mine drainage lagoon. *FEMS Microbiol Rev* 20:351–361.

Cloud, P.E. (1972) A working model of the primitive Earth. *Am J Sci* 272:537–548.

Condie, K.C. (1998) Episodic crustal growth and supercontinents: a mantle avalanche connection. *Earth Planet Sci Lett* 163:97–108.

Cornell, R.M. and Schwertmann, U. (2003) *The Iron Oxides: Structures, Properties, Reactions, Occurrences and Uses,* 2nd ed., Viley-VCH, Weinheim.

Craddock, P.R. and Dauphas, N. (2011) Iron and carbon isotope evidence for microbial iron respiration throughout the Archean. *Earth Planet Sci Lett* 303:121–132.

Croal, L.R., Jiao, Y., Kappler, A., and Newman, D.K. (2009) Phototrophic Fe(II) oxidation in the presence of H_2: implications for banded iron formations. *Geobiology* 7:21–24.

Crowe, S.A., Jones, C., Katsev, S., Magen, C., O'Neill, A.H., Strum, A., Canfield, D.E., Haffner, G.D., Mucci, A., Sundbury, B., and Fowle, D.A. (2008) Photoferrotrophs thrive in an Archean ocean analogue. *Proc Natl Acad Sci USA* 105:15938–15943.

Czaja, A.D., Johnson, C.M., Roden, E.E., Beard, B.L., Voegelin, A.R., Nägler, T.F., Beukes, N.J., and Wille, M. (2012) Evidence for free oxygen in the Neoarchean ocean based on coupled iron–molybdenum isotope fractionation. *Geochim Cosmochim Acta* 86:118–137.

Domagal-Goldman, S.D., Kasting, J.F., Johnston, D.T., and Farquhar, J. (2008) Organic haze, glaciations and multiple sulphur isotopes in the Mid-Archean Era. *Earth Planet Sci Lett* 269:29–40.

Ehrenreich, A. and Widdel, F. (1994) Anaerobic oxidation of ferrous iron by purple bacteria, a new type of phototrophic metabolism. *Appl Environ Microbiol* 60:4517–4526.

Eickhoff, M., Obst, M., Schröder, C., Hitchcock, A.P., Tyliszczak, T., Martinez, R.E., Robbins, L.J., Konhauser, K.O., and Kappler, A. (2014) Nickel partitioning in biogenic and abiogenic ferrihydrite: the influence of silica and implications for ancient environments. *Geochim Cosmochim Acta* 140:65–79.

Eigenbrode, J.L. and Freeman, K.H. (2006) Late Archean rise of aerobic microbial ecosystems. *Proc Natl Acad Sci USA* 103:15759–15764.

Eigenbrode, J.L., Freeman, K.H., and Summons, R.E. (2008) Methylhopane biomarker hydrocarbons in Hamersley Province sediments provide evidence for Neoarchean aerobiosis. *Earth Planet Sci Lett* 273:323–331.

Frierdich, A.J. and Catalano, J.G. (2012) Controls on Fe(II)-activated trace element release from goethite and hematite. *Environ Sci Technol* 46:1519–1526.

Frierdich, A.J., Luo, Y., and Catalano, J.G. (2011) Trace element cycling through iron oxide minerals during redox-driven dynamic recrystallization. *Geology* 39:1083–1086.

Frierdich, A.J., Scherer, M.M., Bachman, J.E., Engelhard, M.H., Rapponotti, B.W., and Catalano, J.G. (2012) Inhibition of trace element release during Fe(II)-activated recrystallization of Al-, Cr-, and Sn-substituted goethite and hematite. *Environ Sci Technol* 46:10031–10039.

Frost, C.D., Blackenburg, F., Schoenberg, R., Frost, B.R., and Swapp, S.M. (2006) Preservation of Fe isotope heterogeneities during diagenesis and metamorphism of banded iron formation. *Contrib Mineral Petrol* 153:211–235.

Godfrey, L.V. and Falkowski, P.G. (2009) The cycling and redox state of nitrogen in the Archaean ocean. *Nat Geosci* 2:725–729.

Gole, M.J. and Klein, C. (1981) Banded iron-formations through much of Precambrian time. *J Geol* 89:169–183.

Grotzinger, J.P. and Knoll, A.H. (1999) Stromatolites in Precambrian carbonates: evolutionary milepost or environmental dipsticks? *Annu Rev Earth Planet Sci* 27:313–358.

Haugaard, R., Frei, R., Stendal, H., and Konhauser, K.O. (2013) Petrology and geochemistry of the ~2.9 Ga Itilliarsuk banded iron formation and associated supracrustal rocks, West Greenland: source characteristics and depositional environment. *Precambrian Res* 229:150–176.

Hayes, J.M., Kaplan, I.R., and Wedeking, K.W. (1983) Precambrian organic geochemistry, preservation of the record. In *Earth's Earliest Biosphere, Its Origin and Evolution*, edited by J.W. Schopf, Princeton University Press, Princeton, NJ, pp 93–134.

Heising, S., Richter, L., Ludwig, W., and Schink, B. (1999) *Chlorobium ferrooxidans* sp. nov., a phototrophic green sulfur bacterium that oxidizes ferrous iron in coculture with a *Geospirillum* sp. strain. *Arch Microbiol* 172:116–124.

Hibbing, M.E., Fuqua, C., Parsek, M.R., and Peterson, S.B. (2010) Bacterial competition: surviving and thriving in the microbial jungle. *Nat Rev Microbiol* 8:15–25.

Hitchcock, A.P., Dynes, J.J., Lawrence, J.R., Obst, M., Swerhone, G.D.W., Korber, D.R., and Leoppard, G.G. (2009) Soft X-ray spectromicroscopy of nickel sorption in a natural river biofilm. *Geobiology* 7:432–453.

Hofmann, A. (2005) The geochemistry of sedimentary rocks from the Fig Tree Group, Barberton greenstone belt: implications for tectonic, hydrothermal and surface processes during mid-Archean times. *Precambrian Res* 143:23–49.

Holland, H.D. (1973) The oceans: a possible source of iron in iron-formations. *Econ Geol* 68:1169–1172.

Holm, N.G. (1989) The $^{13}C/^{12}C$ ratios of siderite and organic matter of a modern metalliferous hydrothermal sediment and their implications for banded iron formations. *Chem Geol* 77:41–45.

Johnson, C.M., Beard, B.L., Klein, C., Beukes, N.J., and Roden, E.E. (2008) Iron isotopes constrain biologic and abiologic processes in banded iron formation genesis. *Geochim Cosmochim Acta* 72:151–169.

Jones, C., Nomosatryo, S., Crowe, S.A., Bjerrum, C.J., and Canfield, D.E. (2015) Iron oxides, divalent cations, silica, and the early earth phosphorus crisis. *Geology* 43:135–138.

Kamber, B.S., Whitehouse, M.J., Bolhar, R., and Moorbath, S. (2005) Volcanic resurfacing and the early terrestrial crust: zircon U-Pb and REE constraints from the Isua greenstone belt, southern West Greenland. *Earth Planet Sci Lett* 240:276–290.

Kappler, A. and Newman, D.K. (2004) Formation of Fe(III)-minerals by Fe(II)-oxidizing photoautotrophic bacteria. *Geochim Cosmochim Acta* 68:1217–1226.

Kappler, A., Pasquero, C., Konhauser, K.O., and Newman, D.K. (2005) Deposition of banded iron formations by anoxygenic phototrophic Fe(II)-oxidizing bacteria. *Geology* 33:865–868.

Kasting, J.F. (2013) What caused the rise of atmospheric O_2? *Chem Geol* 362:13–25.

Kasting, J.F. and Siefert, J.L. (2002) Life and the evolution of Earth's atmosphere. *Science* 296:1066–1068.

Kendall, B., Reinhard, C.T., Lyons, T.W., Kaufman, A.J., Poulton, S.W., and Anbar, A.D. (2010) Pervasive oxygenation along late Archaean ocean margins. *Nat Geosci* 3:647–652.

Kharecha, P., Kasting, J., and Siefert, J. (2005) A coupled atmosphere-ecosystem model of the early Archean Earth. *Geobiology* 3:53–76.

Klein, C. and Beukes, N.J. (1989) Geochemistry and sedimentology of a facies transition from limestone to iron-formation deposition in the Early Proterozoic Transvaal Supergroup, South Africa. *Econ Geol* 84:1733–1774.

Knoll, A.H. (1984) The Archean/Proterozoic transition: a sedimentary and paleobiological perspective. In *Patterns of Change in Earth Evolution*, edited by H.D. Holland, and A.F. Trendall, Springer, Berlin, pp 221–242.

Köhler, I., Konhauser, K.O., and Kappler, A. (2010) Role of microorganisms in banded iron formation. In *Geomicrobiology: Molecular and Environmental Perspective*, edited by L.L. Barton, M. Mandl, and A. Loy, Springer, Berlin, pp 309–324.

Köhler, I., Konhauser, K.O., Papineau, D., Bekker, A., and Kappler, A. (2013) Biological carbon precursor to diagenetic siderite with spherical structures in iron formations. *Nat Commun* 4, doi:10.1038/ncomms2770.

Kolo, K., Konhauser, K.O., Krumbein, W.E., Van Ingelgem, Y., Hubin, A., and Claeys, P. (2009) Microbial dissolution of hematite and associated cellular fossilization by reduced iron phases: a study of ancient microbe-mineral surface interactions. *Astrobiology* 9:777–796.

Konhauser, K.O., Hamade, T., Raiswell, R., Morris, R.C., Ferris, F.G., Southam, G., and Canfield, D.E. (2002) Could bacteria have formed the Precambrian banded iron formations? *Geology* 30:1079–1082.

Konhauser, K.O., Newman, D.K., and Kappler, A. (2005) The potential significance of microbial Fe(III) reduction during deposition of Precambrian banded iron formations. *Geobiology* 3:167–177.

Konhauser, K.O., Amskold, L., Lalonde, S.V., Posth, N.R., Kappler, A., and Anbar, A. (2007a) Decoupling photochemical Fe(II) oxidation from shallow-water BIF deposition. *Earth Planet Sci Lett* 258:87–100.

Konhauser, K.O., Lalonde, S.V., Amskold, L.A., and Holland, H.D. (2007b) Was there really an Archean phosphate crisis? *Science* 315:1234.

Konhauser, K.O., Pecoits, E., Lalonde, S.V., Papineau, D., Nisbet, E.G., Barley, M.E., Arndt, N.T., Zahnle, K., and Kamber, B.S. (2009) Oceanic nickel depletion and a methanogen famine before the Great Oxidation Event. *Nature* 458:750–753.

Konhauser, K.O., Lalonde, S.V., Planavsky, N.J., Pecoits, E., Lyons, T.W., Mojzsis, S.J., Rouxel, O.J., Barley, M.E., Rosiere, C., Fralick, P., Kump, L.R., and Bekker, A. (2011) Aerobic bacterial pyrite oxidation and acid rock drainage during the Great Oxidation Event. *Nature* 478:369–373.

Kump, L.R. and Barley, M.E. (2007) Increased subaerial volcanism and the rise of atmospheric oxygen 2.5 billion years ago. *Nature* 448:1033–1036.

Kurzweil, F., Claire, M., Thomazo, C., Peters, M., Hannington, M., and Strauss, H. (2013) Atmospheric sulphur rearrangement 2.7 billion years ago: evidence for oxygenic photosynthesis. *Earth Planet Sci Lett* 366:17–26.

Lalonde, S.V. and Konhauser, K.O. (2015) Benthic perspective on Earth's oldest evidence for oxygenic photosynthesis. *Proc Natl Acad Sci USA* 112:995–1000.

Large, R.R., Halpin, J.A., Danyushevsky, L.V., Maslennikov, V.V., Bull, S.W., Long, J.A., Gregory, D.D., Lounejeva, E., Lyons, T.W., Slack, P.J., McGoldrick, P.J., and Claver, C.R. (2014) Trace element content of sedimentary pyrite as a new proxy for deep-time ocean-atmosphere evolution. *Earth Planet Sci Lett* 389:309–220.

Li, W., Huberty, J.M., Beard, B.L., Kita, N.T., Valley, J.W., and Johnson, C.M. (2013) Contrasting behavior of oxygen and iron isotopes in banded iron formations revealed by *in situ* isotopic analysis. *Earth Planet Sci Lett* 384:132–143.

Li, Y.-L., Konhauser, K.O., Cole, D.R., and Phelps, T.J. (2011) Mineral ecophysiological data provide growing evidence for

microbial activity in banded-iron formations. *Geology* 39:707–710.

Li, Y.-L., Konhauser, K.O., Kappler, A., and Hao, X.-L. (2013) Experimental low-grade alteration of biogenic magnetite indicates microbial involvement in generation of banded iron formations. *Earth Planet Sci Lett* 361:229–237.

Londry, K.L., Dawson, K.G., Grover, H.D., Summons, R.E., and Bradley, A.S. (2008) Stable carbon isotope fractionation between substrates and products of *Methanosarcina barkeri*. *Org Geochem* 39:608–621.

McNamara, K.J. and Awramik, S.M. (1992) Stromatolites: a key to understanding the early evolution of life. *Sci Prog* 76:345–364.

Moon, E.M. and Peacock, C.L. (2012) Adsorption of Cu(II) to ferrihydrite and ferrihydrite-bacteria composites: importance of the carboxyl group for Cu mobility in natural environments. *Geochim Cosmochim Acta* 92:203–219.

Moon, E.M. and Peacock, C.L. (2013) Modelling Cu(II) adsorption to ferrihydrite and ferrihydrite-bacteria composites: deviation from additive adsorption in the composite sorption system. *Geochim Cosmochim Acta* 104:148–164.

Morris, R.C. (1993) Genetic modelling for banded iron-formation of the Hamersley Group, Pilbara Craton, Western Australia. *Precambrian Res* 60:243–286.

Muehe, E.M., Scheer, L., Daus, B., and Kappler, A. (2013) Fate of arsenic during microbial reduction of biogenic versus abiogenic As-Fe(III)-mineral coprecipitates. *Environ Sci Technol* 47:8297–8307.

Pantke, C., Obst, M., Benzerara, K., Morin, G., Ona-Nguema, G., Dippon, U., and Kappler, A. (2012) Green rust formation during Fe(II) oxidation by the nitrate-reducing *Acidovorax* sp. strain BoFeN1. *Environ Sci Technol* 46:1439–1446.

Parmar, N., Gorby, Y.A., Beveridge, T.J., and Ferris, F.G. (2001) Formation of green rust and immobilization of nickel in response to bacterial reduction of hydrous ferric oxide. *Geomicrobiol J* 18:375–382.

Pavlov, A.A., Kasting, J.F., Brown, L.L., Rages, K.A., and Freedman, R. (2000) Greenhouse warming by CH_4 in the atmosphere of early Earth. *J Geophys Res* 105:11981–11990.

Pavlov, A.A., Kasting, J.F., Eigenbrode, J.L., and Freeman, K.H. (2001) Organic haze in Earth's early atmosphere: source of low-^{13}C late Archean kerogens? *Geology* 29: 1003–1006.

Pecoits, E., Gingras, M.K., Barley, M.E., Kappler, A., Posth, N.R., and Konhauser, K.O. (2009) Petrography and geochemistry of the Dales Gorge banded iron formation: paragenetic sequence, source and implications for palaeo-ocean chemistry. *Precambrian Res* 172:163–187.

Pecoits, E., Smith, M.L., Catling, D.C., Philippot, P., Kappler, A., and Konhauser, K.O. (2015) Atmospheric hydrogen peroxide and Eoarchean iron formations. *Geobiology* 13:1–14.

Perry, E.C., Tan, F.C., and Morey, G.B. (1973) Geology and stable isotope geochemistry of the Biwabik Iron Formation, Northern Minnesota. *Econ Geol* 68:1110–1125.

Planavsky, N.J., Rouxel, O., Bekker, A., Lalonde, S.V., Konhauser, K.O., Reinhard, C.T., and Lyons, T. (2010) The evolution of the marine phosphate reservoir. *Nature* 467:1088–1090.

Planavsky, N., Rouxel, O.J., Bekker, A., Hofmann, A., Little, C.T.S., and Lyons, T.W. (2012) Iron isotope composition of some Archean and Proterozoic iron formations. *Geochim Cosmochim Acta* 80:158–169.

Popp, B.N., Laws, E.A., Bidigare, R.R., Dore, J.E., Hanson, K.L., and Wakeham, S.G. (1998) The effect of phytoplankton cell geometry on carbon isotopic fractionation. *Geochim Cosmochim Acta* 62:69–77.

Posth, N., Hegler, F., Konhauser, K.O., and Kappler, A. (2008) Ocean temperature fluctuations as trigger for Precambrian Si and Fe deposition. *Nat Geosci* 1:703–707.

Posth, N.R., Huelin, S., Konhauser, K.O., and Kappler, A. (2010) Size, density and composition of cell-mineral aggregates formed during anoxygenic phototrophic Fe(II) oxidation: impact on modern and ancient environments. *Geochim Cosmochim Acta* 74:3476–3493.

Posth, N.R., Konhauser, K.O., and Kappler, A. (2013a) Microbiological processes in banded iron formation deposition. *Sedimentology* 60:1733–1754.

Posth, N.R., Köhler, I., Swanner, E.D., Schröder, C., Wellmann, E., Binder, B., Konhauser, K.O., Neumann, U., Berthold, C., Nowak, M., and Kappler, A. (2013b) Simulating Precambrian banded iron formation diagenesis. *Chem Geol* 362:66–73.

Poulton, S.W., Fralick, P.W., and Canfield, D.E. (2004) The transition to a sulphidic ocean $\sim$1.84 billion years ago. *Nature* 431:173–177.

Rasmussen, B., Krapež, B., Muhling, J.R., and Suvorova, A. (2015) Precipitation of iron silicate nanoparticles in early Precambrian oceans marks Earth's first iron age. *Geology* 43:303–306.

Reinhard, C.T., Raiswell, R., Scott, C., Anbar, A.D., and Lyons, T.W. (2009) A Late Archean sulfidic sea stimulated by early oxidative weathering of the continents. *Science* 326:713–716.

Robbins, L.J., Lalonde, S.V., Saito, M.A., Planavsky, N.J., Mloszewska, A.M., Pecoits, E., Scott, C., Dupont, C.L., Kappler, A., and Konhauser, K.O. (2013) Authigenic iron oxide proxies for marine zinc over geological time and implications for eukaryotic metallome evolution. *Geobiology* 11:295–306.

Robbins, L.J., Swanner, E.D., Lalonde, S.V., Eickhoff, M., Paranich, M.L., Reinhard, C.T., Peacock, C.L., Kappler, A., and Konhauser, K.O. (2015) Limited Zn and Ni mobility during simulated iron formation diagenesis. *Chem Geol* 402:30–39.

Robinson, J.J., Scott, K.M., Swanson, S.T., O'Leary, M.H., Horken, K., Tabita, F.R., and Cavanaugh, C.M. (2003) Kinetic isotope effect and characterization of form II RubisCO from chemoautotrophic endosymbionts of the hydrothermal vent tubeworm *Riftia pachyptila*. *Limnol Oceanogr* 48:48–54.

Smithies, R.H., Van Kranendonk, M.J., and Champion, D.C. (2005) It started with a plume—early Archaean basaltic proto-continental crust. *Earth Planet Sci Lett* 238:284–297.

Steinhoefel, G., von Blanckenburg, F., Horn, I., Konhauser, K.O., Beukes, N.J., and Gutzmer, J. (2010) Deciphering formation processes of banded iron formations from the Transvaal and the Hamersley successions by combined Si and Fe isotope analysis using UV femtosecond laser ablation. *Geochim Cosmochim Acta* 74:2677–2696.

Sumner, D.Y. (1997) Carbonate precipitation and oxygen stratification in late Archean seawater as deduced from facies and stratigraphy of the Gamohaan and Frisco formations, Transvaal Supergroup, South Africa. *Am J Sci* 297:455–487.

Sumner, D.Y. and Beukes, N.J. (2006) Sequence stratigraphic development of the Neoarchean Transvaal carbonate platform, Kaapvaal Craton, South Africa. *South Afr J Geol* 109:11–22.

Sun, S., Konhauser, K.O., Kappler, A., and Li, Y.-L. (2015) Primary hematite in Neoarchean to Paleoproterozoic oceans. *Geol Soc Am Bull* 127:850–861.

Swanner, E.D., Mloszewska, A.M., Cirpka, O.A., Schoenberg, R., Konhauser, K.O., and Kappler, A. (2015) Modulation of oxygen production in Archaean oceans by episodes of Fe(II) toxicity. *Nat Geosci* 8:126–130.

Toner, B.M., Berquó, T.S., Michel, F.M., Sorensen, J.V., Templeton, A., and Edwards, K.J. (2012) Mineralogy of iron microbial mats from Loihi Seamount. *Front Microbiol* 3, doi:10.3389/fmicb.2012.0018.

Trolard, F., Génin, J.-M.R., Abdelmoula, M., Bourrié, G., Humbert, B., and Herbillon, A. (1997) Identification of a green rust mineral in a reductomorphic soil by Mössbauer and Raman spectroscopies. *Geochim Cosmochim Acta* 61:1107–1111.

Ueno, Y., Yamada, K., Yoshida, N., Maruyama, S., and Isozaki, Y. (2006) Evidence from fluid inclusions for microbial methanogenesis in the early Archaean era. *Nature* 440:516–519.

Wade, J. and Wood, B.J. (2005) Core formation and the oxidation state of the Earth. *Earth Planet Sci Lett* 236:78–95.

Walker, J.C.G. (1984) Suboxic diagenesis in banded iron formations. *Nature* 309:340–342.

Weber, M.F., Poxleitner, G., Hebisch, E., Frey, E., and Opitz, M. (2014) Chemical warfare and survival strategies in bacterial range expansions. *J R Soc Interface* 11, 10.1098/rsif.2014.0172.

Widdel, F., Schnell, S., Heising, S., Ehrenreich, A., Assmus, B., and Schink, B. (1993) Ferrous iron oxidation by anoxygenic phototrophic bacteria. *Nature* 362:834–836.

Wu, W., Swanner, E.D., Hao, L., Zeitvogel, F., Obst, M., Pan, Y., and Kappler, A. (2014) Characterization of the physiology and cell-mineral interactions of the marine anoxygenic phototrophic Fe(II)-oxidizer *Rhodovulum iodosum*—implications for Precambrian banded iron formation deposition. *FEMS Microbiol Ecol* 3:503–515.

Zahnle, K.J., Claire, M.W., and Catling, D.C. (2006) The loss of mass-independent fractionation of sulfur due to a Paleoproterozoic collapse of atmospheric methane. *Geobiology* 4:271–283.

Zegeye, A., Bonneville, S., Benning, L.G., Strum, A., Fowle, D.A., Jones, C., Canfield, D.E., Ruby, C., MacLean, L.C., Nomosatryo, S., Crowe, S.A., and Poulton, S.W. (2012) Green rust formation controls nutrient availability in a ferruginous water column. *Geology* 40:599–602.

Zerkle, A.L., Claire, M., Domagal-Goldman, S.D., Farquhar, J., and Poulton, S.W. (2012) A bistable organic-rich atmosphere on the Neoarchaean Earth. *Nat Geosci* 5:359–363.

Address correspondence to:
Kurt O. Konhauser
Department of Earth and Atmospheric Sciences
University of Alberta
3-13 ESB Building
Edmonton, Alberta T6G2E3
Canada

E-mail: kurtk@ualberta.ca

Submitted 11 February 2015
Accepted 24 May 2015

Abbreviations Used

GOE = Great Oxidation Event
IF = iron formations
SRB = sulfate-reducing bacteria
STXM = scanning transmission X-ray microscopy